Bitlis Eren Üniversitesi Fen Bilimleri Dergisi
BİTLİS EREN UNIVERSITY JOURNAL OF SCIENCE
ISSN: 2147-3129/e-ISSN: 2147-3188
VOLUME: 13 NO: 2 PAGE: 432-444 YEAR: 2024
DOI:10.17798/bitlisfen.1421143

# Effect of Chain-Link Fence Attachment on the Crash Performance of an H1 Containment Level Safety Barrier

Ayhan Öner YÜCEL[1*]

[1]*Aydın Adnan Menderes University, Faculty of Engineering, Department of Civil Engineering, Aydın, Türkiye*
*(ORCID: 0000-0001-5888-2809)*

**Keywords:** Longitudinal barrier, Crash simulation, Finite element Analysis, Chain-link fence, EN 1317.

**Abstract**
Longitudinal barriers are among the road safety equipment used to prevent vehicles from leaving the roadway. These systems are designed to be lightweight for economic reasons without compromising their structural adequacy. In this study, the effect of chain-link fence on impact severity and structural performance of a longitudinal barrier was investigated through finite element (FE) analyses. An H1 containment level longitudinal barrier FE model was validated using real crash test results. After modifying the validated system to reduce its weight, crash test simulations (TB11 and TB42) were conducted on the modified system, both with and without chain-link fence attachment. The chain-link fence was placed below the rail and on the traffic side of the post in a manner that had not been applied before. FE analyses found that the chain-link fence minimally altered TB11 test performance. In TB42 simulations without a chain-link fence, the vehicle climbed over the rail, resulting in a test failure. However, when a chain-link fence was used, the same barrier contained and redirected the vehicle, leading to a successful test. It was concluded that using chain-link fences can enhance the crash performance of longitudinal barriers by limiting the barrier lateral deformation. Further detailed studies, supported by real crash tests, on the placement of fences in barriers are recommended.

## 1. Introduction

Longitudinal barriers designed in accordance with the European EN 1317 standard offer specific levels of vehicle containment, effectively redirecting errant vehicles back onto the road [1]. Crash tests are conducted on safety barriers to evaluate their performance levels, with the goal of ensuring that these barriers are structurally adequate and have minimal injury risk to occupants. Different types of longitudinal barriers are grouped by how well they resist deformation. For example, concrete barriers are rigid, steel barriers are semi-rigid when it comes to lateral deformation, and cable barriers are flexible. The focus of this study was on steel barriers. The performance of safety barriers is notably impacted by their geometric features, as highlighted in studies by Molan et al. [2] and Molan and Ksaibati [3]. Key parameters such as barrier height and post spacing play a crucial role in ensuring safety performance [4]. Additionally, the severity of the impact is significantly influenced by both the type and material of the post [4], [5]. The increase in vehicle weights, attributed to the use of batteries in electric vehicles, and the desire to employ lower-cost road restraint systems have prompted researchers to design lightweight, higher-performance systems that prioritize structural adequacy and occupant safety.

Chain-link fences are commonly used systems for various purposes, such as protection against rockfall, debris flows, and security. Recently, their usage of road restraint systems has increased. Silvestri-Dobrovolny et al. [6] evaluated the crash performance of a chain-link fence fixed on the top of

*Corresponding author: aoyucel@adu.edu.tr
*Received: 17.01.2024, Accepted: 03.06.2024*

concrete barriers. They are generally used to deter pedestrians from crossing. According to that study, chain-link fence systems are installed at the top or back of concrete barriers in the United States. The general purpose of mounting a chain-link fence is to prevent people from passing or jumping from the barrier in the median or on bridges. The advantages of chain-link fence attachments were listed as easy attachment, withstanding wind loads, and compatibility with MASH. The disadvantage was listed as limited glare screening. A real full-scale crash test was implemented according to MASH Test 3-11 for an F-shape concrete barrier with a chain-link fence mounted on the top [7]. A 2270-kg truck impacted the barrier at a speed of 100 km/h and at an angle of 25°. The system successfully passed the test. Literature reviews showed that there is no study (real crash test or FE analyses) regarding the crashworthiness of longitudinal steel barriers with chain-link fence attachments. In another study, Silvestri Dobrovolny et al. [8] developed and evaluated barrier containment options for the safety of motorcycle riders. They designed a concrete barrier with a chain-link fence mounted on top to decrease the severity of motorcycle crashes. Finite element computer simulations were implemented to evaluate the concrete barrier with chain-link fence attachment. According to FE simulations, the developed system successfully contained the dummy with the help of a mounted chain-link fence system.

Due to the time-consuming and expensive nature of real crash tests, as well as the need for extensive technical infrastructure, the use of finite elements in the crashworthiness evaluation of road restraint systems has become widespread with advancements in computer technologies. Numerous studies have investigated the crash performance of road safety systems through FE analyses [9]-[13]. A 3D finite element model of a chain-link drapery system was developed in ABAQUS software [14]. Real-impact tests in the lab were used to calibrate and validate the model. These tests showed that the FE model accurately depicts the behavior of the chain-link drapery system. Similarly, a chain-link fence finite element model was developed and validated for simulations with the LS-DYNA [8]. They modeled the fence using beam elements and validated the model with real pendulum tests. The results indicated that the FE model of the chain-link fence accurately represents its actual impact behavior. Another chain-link fence FE model was developed by Hoang et al. [15]. They simulated protective fences against rockfalls. The results of the pendulum tests and LS-DYNA outputs were very similar, showing that FE analyses can be used to accurately model the fence's changing behavior.

The primary objective of this study is to investigate the impact of chain-link fence placement in longitudinal barriers on crash performance. Within the scope of this research, an H1 containment level barrier FE model was developed and validated using actual crash test results. The reference model underwent modifications to reduce the system's weight. TB11 and TB42 crash simulations were conducted using LS-DYNA software for the modified barrier system, both with and without chain-link fence placement. The study assessed the influence of chain-link fence usage on the performance of the modified barrier system, with evaluations focusing on the impact severity on passengers and the structural adequacy of the barrier. The findings of this study could be useful for evaluating the potential use of chain-link fences with longitudinal barriers.

## 2. Material and Method

### 2.1. Longitudinal Barrier Performance Evaluation according to EN 1317

Before road restraint systems are used on European highways, they must undergo testing and certification according to the European standard EN 1317 to assess their crashworthiness [1]. This standard describes test details for different barrier performance classes and certification procedures. EN 1317 comprises eight separate parts, with the first two covering crash test procedures, test vehicle criteria, and general specifications for longitudinal barriers. Terminology, general criteria, and test vehicle specifications are outlined in EN 1317-1 [16]. EN 1317-2 defines test methods for different performance classes and acceptance criteria [1]. This standard delineates containment levels, ranging from low-angle containment to very high containment, along with the required acceptance tests. It describes a total of eleven crash tests involving different vehicle types, masses, impact speeds, and impact angles. In the scope of this study, an H1 containment level steel longitudinal barrier, classified as a higher containment level, was utilized. As indicated in Table 1, TB11 and TB42 crash tests must be conducted for H1 level acceptance. The crash test results must meet EN 1317-2 criteria for successful certification. The TB11 test is performed using a 900 kg car, with the car impacting the barrier at a speed of 100 km/h and at an angle of 20°. The TB42 test involves a rigid Heavy Goods Vehicle (HGV) weighing 10000 kg colliding with the barrier at a speed of 70 km/h and at an angle of 15°.

**Table 1.** The details of tests required for H1 containment level [1]

| Containment level | | Required Test | Speed (km/h) | Angle (°) | Mass (kg) | Type of vehicle |
|---|---|---|---|---|---|---|
| Higher containment | H1 | TB11 | 100 | 20 | 900 | Car |
| | | TB42 | 70 | 15 | 10000 | Rigid HGV |

After conducting full-scale real crash tests, the results are evaluated based on EN 1317-2 specifications. Crash test outcomes are assessed considering the structural adequacy of the barrier, occupant impact severity, and vehicle trajectory. The barrier must meet EN 1317 criteria, including occupant impact severity levels in the car test (TB11), structural adequacy in the HGV test (TB42), and vehicle stability requirements during both tests. In a successful crash test, the vehicle should not roll over, and must be contained and redirected to the traffic side of the barrier, and there should be no complete breakage in the main longitudinal components of barrier system [1]. Within the scope of this study, both the TB11 and TB42 crash test results were investigated. TB11 test results are utilized to assess the impact severity level. The acceleration severity index (ASI) and the theoretical head impact velocity (THIV) indices are employed to quantify the injury risk of vehicle occupants. The ASI reflects impact intensity and is calculated using the accelerations measured during the crash test. The THIV estimates the velocity of the occupant's head during an impact. According to the EN 1317 standard, ASI is determined using Equation (1).

$$ASI(t) = max\left[\sqrt{\left[\left(\frac{a_x}{\hat{a}_x}\right)^2 + \left(\frac{a_y}{\hat{a}_y}\right)^2 + \left(\frac{a_z}{\hat{a}_z}\right)^2\right]}\right] \quad (1)$$

where, $a_x$, $a_y$ and $a_z$ are the acceleration values obtained during the crash testing (measured in g, where g is gravitational acceleration). $\hat{a}_x$, $\hat{a}_y$ and $\hat{a}_z$ refers to limit acceleration values in the longitudinal (x), lateral (y), and vertical (z) directions, respectively. These limit accelerations are given as 12 g, 9 g, and 10 g, respectively.

The THIV index is calculated using the velocities of the theoretical head with respect to the car. The equation used to calculate THIV is given in Equation (2).

$$THIV = \left[V_{head\,x}^2(T) + V_{head\,y}^2(T)\right]^{0.5} \quad (2)$$

where, $V_{head\,x}$ and $V_{head\,y}$ refer to the head velocity with respect to the car in the longitudinal and lateral directions of the vehicle coordinate system, respectively. T refers to the time of flight required for theoretical head displacement, either 600 mm in the x direction or 300 mm in the y direction.

EN 1317-2 establishes ASI and THIV limit values as shown in Table 2 [1]. The impact severity level is determined according to the given ASI ranges. THIV value must be less than 33 km/h for the acceptance of the test in terms of occupant safety. The lower ASI values are desired for reduced impact severity.

**Table 2.** Impact severity levels according to EN 1317-2 [1]

| Impact severity level | Characteristic values | | |
|---|---|---|---|
| A | ASI ≤ 1.0 | | |
| B | 1.0 < ASI ≤ 1.4 | and | THIV < 33 km/h |
| C | 1.4 < ASI ≤ 1.9 | | |

In addition to safety criteria, the structural adequacy of the barrier is crucial for acceptance. The TB42 test is conducted to evaluate the structural performance of H1 containment level barriers. The working width (W) is defined as the maximum lateral deformation of the safety barrier during the crash test. It is measured during the test as the greatest lateral distance between the impact side of the safety barrier and any part of the barrier during the impact. Table 3 presents the working width ranges and corresponding classes.

**Table 3.** Working width classes [1]

| Class | Working width (m) |
|---|---|
| W1 | W≤0.6 |
| W2 | W≤0.8 |
| W3 | W≤1.0 |
| W4 | W≤1.3 |
| W5 | W≤1.7 |
| W6 | W≤2.1 |
| W7 | W≤2.5 |
| W8 | W≤3.5 |

Exit box criteria must also be taken into consideration according to EN 1317 [1]. According to these criteria, all vehicles should be redirected to the road platform at a small angle by the safety barrier after the impact. If the exit angle is large, the errant vehicle may pose a safety risk to other vehicles in the traffic lanes. Following the crash test, the vehicle exit angle and

exit box criteria should be checked against the limits specified for vehicle dimensions.

### 2.2. Geometric details and Finite Element (FE) Model of Reference H1 Containment Level Barrier

In this study, a previously tested and certified H1 containment level longitudinal barrier served as a reference system. This system underwent modification and analysis to investigate the impact of chain-link fence placement on its performance. The original safety barrier comprises two main components: C-type posts and W-beam rails. Bolts and nuts are utilized to connect the rails to each other and to attach the rails to the posts. The W-beam rails, made of 2.65 mm thick steel, are connected to 5 mm thick steel C150X75 posts using M16 bolts. Figure 1 illustrates the geometric details of barrier components. The total length of the posts is 1600 mm, with 810 mm embedded into the ground. Consequently, the total height of the post above the ground is 790 mm. The distance between each post in this system is 2 meters. The material grade for the W-beam is S235JR, while the C-type post has a material grade of S355JR. The M16 bolts are composed of Class 8.8 steel material. This H1 safety barrier underwent TB11 and TB42 crash tests in real full-scale conditions, conducted at an accredited crash test center located in France [17], [18].

The finite element (FE) model of the barrier system was created for validation and subsequent analyses. The general view of the H1 containment level safety barrier FE model is illustrated in Figure 2. The 3-dimensional nonlinear finite element software LS-DYNA was used for crash analyses [19]. LS-PrePost software was used to define element types, material models, and other details during the model creation phase. In the development of the FE model, the material properties and geometries of the barrier components were defined to accurately reflect the real crash test results. Rail and post models were created using shell element types. The material properties of steel elements were defined in LS-DYNA using the MAT024 (piecewise linear plasticity) material model. To represent the M16 bolt connection between the post and rail, beam elements were defined. The material properties and failure criteria were established based on the material class of bolts using the MAT098 (simplified Johnson cook) material model. The failure definition in beam connections ensures that the parts remain connected until a certain stress criterion is met. After reaching the limit, the connection fails, and members move freely. Contact definitions between barrier components were established.

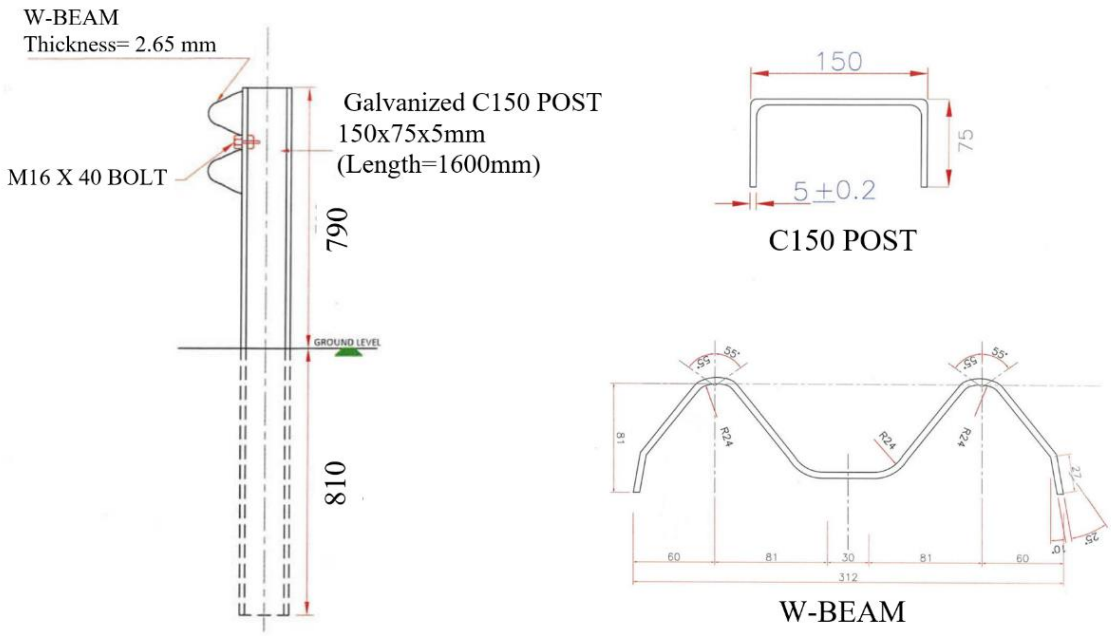


**Figure 1.** The geometric details of H1 containment level safety barrier studied [18]

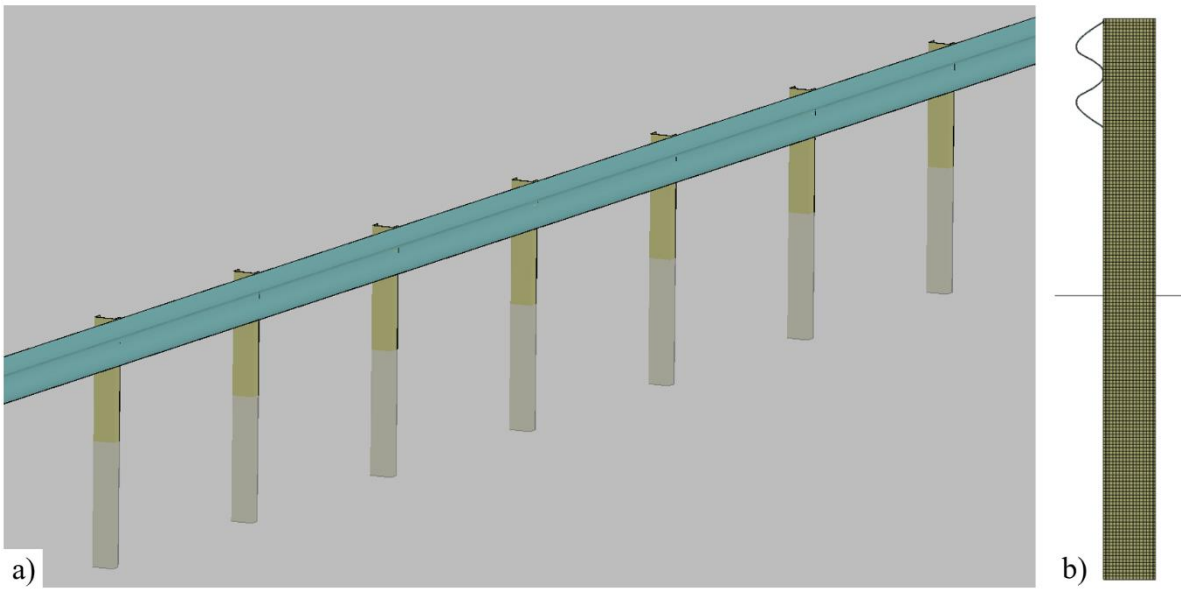


**Figure 2.** The FE model of H1 barrier system: a) General view, b) Side view (mesh view is on)

### 2.3. Validation of Finite Element (FE) Model

The safety barrier FE model must undergo validation using real crash test data before being utilized for further analyses. The barrier performance in the virtual testing should closely align with real-world results to validate the FE model. In this study, the validation and verification process for virtual testing followed the error tolerances outlined in the European standard EN 16303 [20]. To validate the FE model, variations in the test results, such as working width, should be within acceptable limits defined by the standard. Once validated, the model is deemed ready for subsequent crash simulations. Validation was performed using actual full-scale TB42 crash test results. Subsequently, a full-scale FE model for the H1 barrier system under TB42 test conditions was created using LS-DYNA. As previously mentioned, the TB42 test involves a 10000 kg HGV impacting the barrier at a speed of 70 km/h and an angle of 15°. The 10000 kg HGV FE model, developed and validated by the National Crash Analysis Center, was employed [21]. Vehicle and barrier models were integrated into a main file, and their positions were adjusted in accordance with EN 1317-2 and the real crash test conditions. Parameters such as vehicle initial velocity, contacts between vehicle and barrier components, and frictions between surfaces were defined. Additionally, parameters for test outputs, such as the test termination time and plot time intervals, were defined. Figure 3 provides an overview of both the actual full-scale TB42 crash test's initial condition and the corresponding FE model.

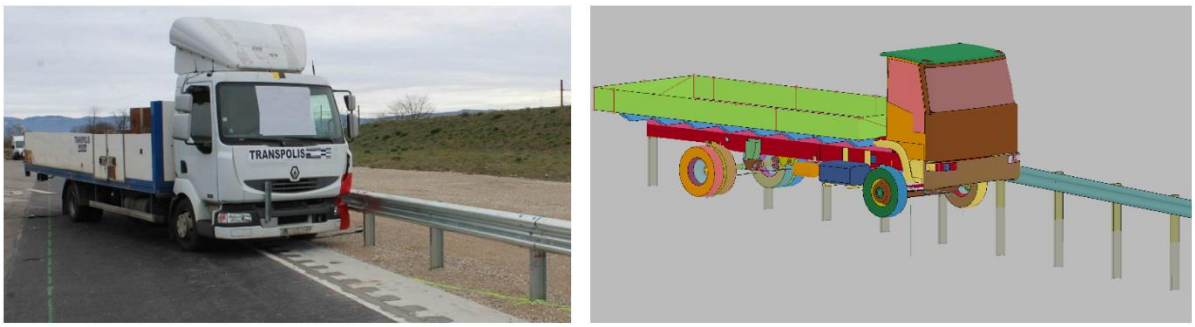


**Figure 3.** General overview of TB42 test before crash: real test (left) [18], FE model (right)

The actual test and FE analysis results were compared for validation. Working width results were compared according to the EN 16303 standard. In the real test, the working width of the barrier ($W_m$) was determined to be 1.14 mm, corresponding to the W4 class. EN 16303 mandates the comparison of working widths between the physical test ($W_m$) and the virtual test ($W_{VT}$). The difference between these two working widths must be less than the calculated value, according to Equation (3).

$$|W_m - W_{VT}| \leq \left(0.1 + 0.1 \times (D_m)\right) \quad (3)$$

where, $W_m$ is the working width of the real test (m), $W_{VT}$ is the working width of the virtual test (m), and $D_m$ is the dynamic deflection of the actual barrier (m). In the virtual test, the working width was determined to be 1.07 m, resulting in a difference of 0.07 m compared to the actual working width of 1.14 m in the real test. The dynamic deflection of the barrier ($D_m$) in the real test was measured to be 1.09 m. Calculating the right-hand side of the equation yielded 0.209 m. As this difference between the working widths was less than the limit value of 0.209 m, the FE model satisfied the working width criteria of EN 16303.

Figure 4 provides a side-by-side comparison between the real crash test and the FE simulation. The collision occurred at a 15° angle with a velocity of about 70 km/h. In the actual test, the collision took place near the 10$^{th}$ post, resulting in the deformation of posts 10-18 during the impact. Approximately 0.52 seconds after the initial impact, the vehicle aligned parallel to the barrier. Although the vehicle moved forward for a while due to wheel movement caused by the collision, it eventually came to a stop without leaving the barrier. The exit angle and exit box criteria in EN 1317-2 were met in this test.

The maximum lateral deformations in barriers during the real crash test and FE analysis are depicted in Figure 5. The strong correlation between the FE simulation and actual crash test outcomes is evident. The validation results confirm the suitability of the FE model for subsequent analyses in this study.

According to real TB11 crash test results, the working width was determined as 0.73 m, and the ASI and THIV parameters were obtained as 1.0 and 23 km/h, respectively [17]. These results led to the certification of this barrier system as an H1-W4-A system.

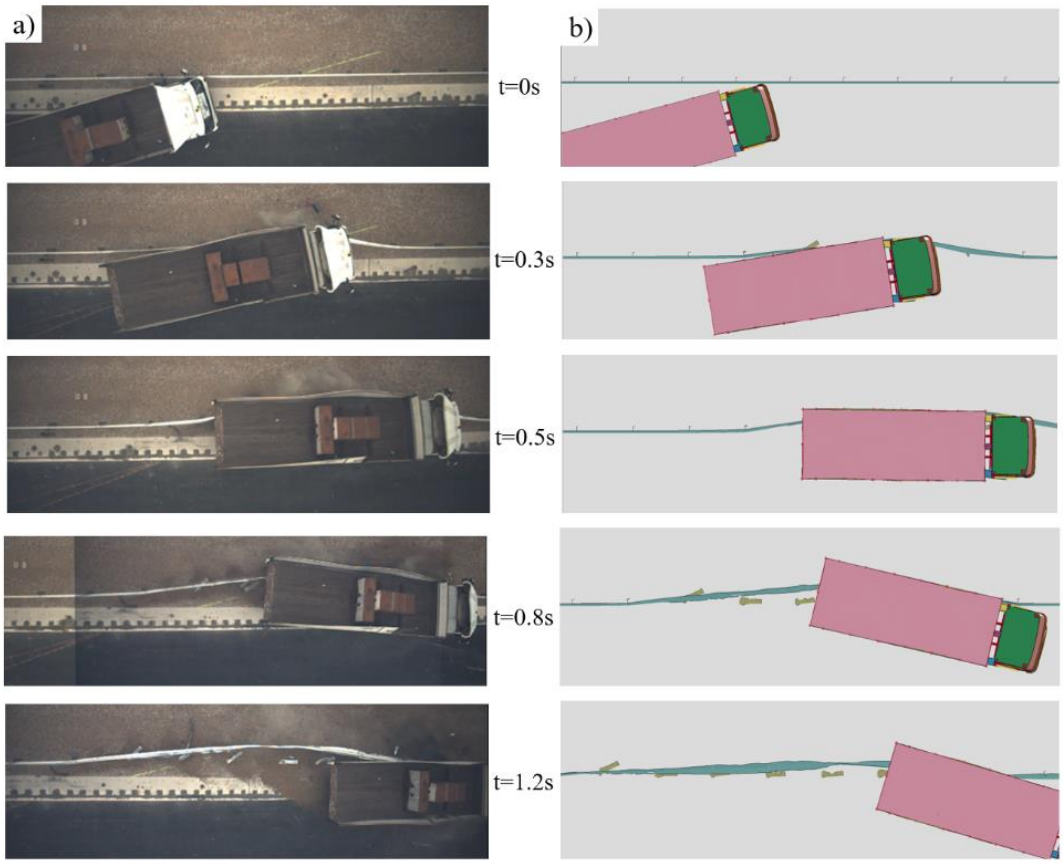


**Figure 4.** Comparison of TB42 results: a) Actual crash test [18], b) FE simulation

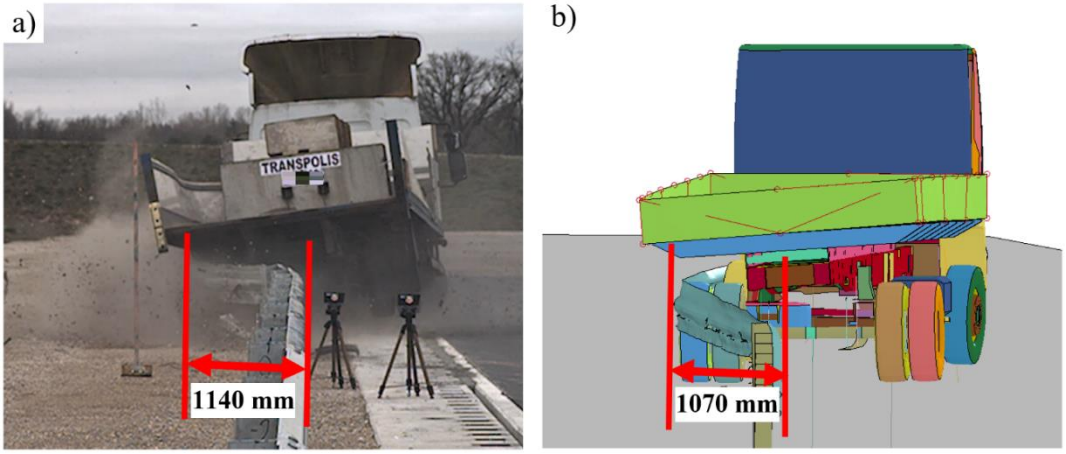


**Figure 5.** Comparison of barrier deformations: a) Full-scale crash test [18], b) FE simulation

## 2.4. Modified Barrier System and Fence Attachment

In this study, the tested and certificated H1-W4-A longitudinal barrier underwent modifications to reduce its weight. The investigation aimed to assess the impact of chain-link fence attachment on barrier performance and vehicle behavior. Analyses were conducted for the modified system, both with and without fence attachment. The 150x75 post and W-beam rail steel material properties remained the same as the reference initial H1-W4-A system, but their thickness was reduced to decrease the overall system weight. The original post length was 1600 mm, with 810 mm in the ground and the remaining 790 mm above the surface. In the modified system, the post length was reduced to 1500 mm, with 800 mm below the ground and 700 mm above the ground. The thickness of the posts, originally 5 mm, was reduced to 4 mm. The W-beam rail thickness decreased from 2.65 mm to 2.5 mm. Additionally, the post-rail connection bolts, initially M16-Class 8.8 bolts, were updated to M10-Class 4.6. The rail and post connections were set 160 mm below the upper end of the posts. While the weight of the reference barrier system's 1 m length was approximately 19.1 kg, the modified barrier system's weight was reduced to about 16.3 kg per 1 m length. To conduct FE analysis of the modified system, its FE model was created, as illustrated in Figure 6. Geometric details and dimensions are indicated in this figure.

In previous applications involving chain-link fences, they were utilized by fixing them to the top of longitudinal barriers. This was done to protect motorcycle drivers or prevent pedestrian crossings on highways. However, in this study, a different approach was taken. A chain-link fence was attached to the modified barrier system between the W-beam rail and post. The effects of this configuration on barrier performance were investigated through finite element analyses. Figure 7 provides a typical representation of the chain-link fence appearance.

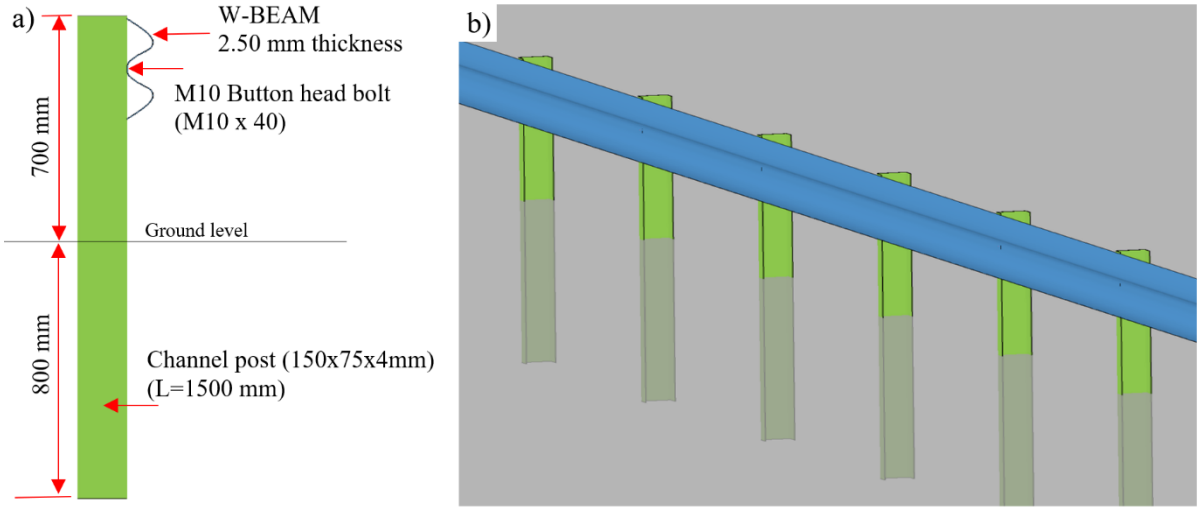


**Figure 6.** FE model of modified barrier system without fence: a) Side view, b) General view

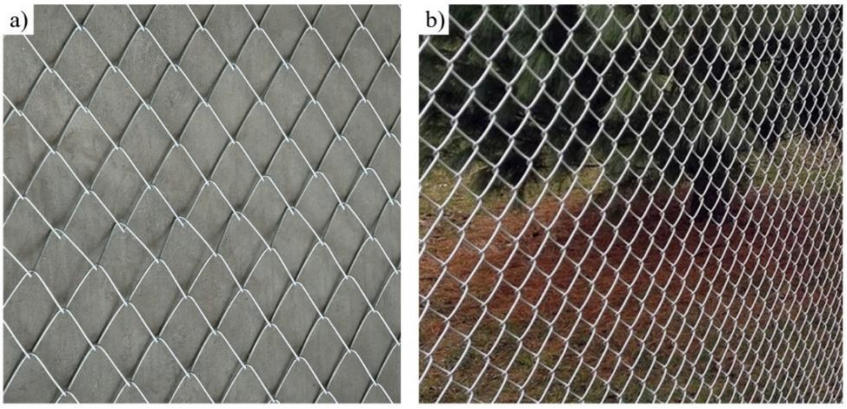


**Figure 7.** The typical view of chain-link fence: a) Example-1 [22], b) Example-2 [23]

In this study, a chain-link fence made from hot-dip galvanized wire material was incorporated into the finite element model preparation. The wire material's properties, produced in accordance with the TS EN 10223-6 standard, were utilized and defined in the FE model [24]. The chosen wire diameter for the chain-link fence was 2.5 mm, with a mesh size of 50 mm x 50 mm. Commonly used wire materials for chain-wire production in Turkey exhibit a minimum tensile strength of 350 N/mm$^2$, and the general material tensile strength falls within the range of 350-750 N/mm$^2$ [22], [25]. Material properties for the chain-link fence in the LS-DYNA model were defined using the MAT024 (piecewise linear plasticity) material model, selecting a tensile strength of 500 N/mm$^2$ and specifying other relevant properties. To model the steel wires, beam elements were used. The chain-link fence was longitudinally positioned between the rail and the post elements, facilitated by rectangular plates. Geometric details and the location of the chain-link fence are depicted in Figure 8. The lower edge of the fence is positioned 100 mm above the ground, with a fence height of 460 mm. A 450x70x3 (mm) steel support plate, made of S235JR grade material, secures the chain-link fence to the system using two bolts. The upper part of this plate is sandwiched between the post and the rail, utilizing the post-rail connection bolt. The lower part of the plate is connected to the post with a second M10-Class 4.6 bolt. The addition of the fixing plate increased the system weight to approximately 16.7 kg per 1m. Additionally, around 0.8 kg of chain-link fence is used in the 1 m barrier system.

To assess the impact severity and barrier structural performance with the inclusion of a chain-link fence, TB11 and TB42 FE simulations were conducted for both the modified system without a fence and the modified system with a fence. A total of four FE analyses were executed using LS-DYNA software. The validated barrier FE model underwent modifications specific to these tests. Vehicle FE models were obtained from the National Crash Analysis Center [21]. The general view of the models before the crash analyses is illustrated in Figure 9.

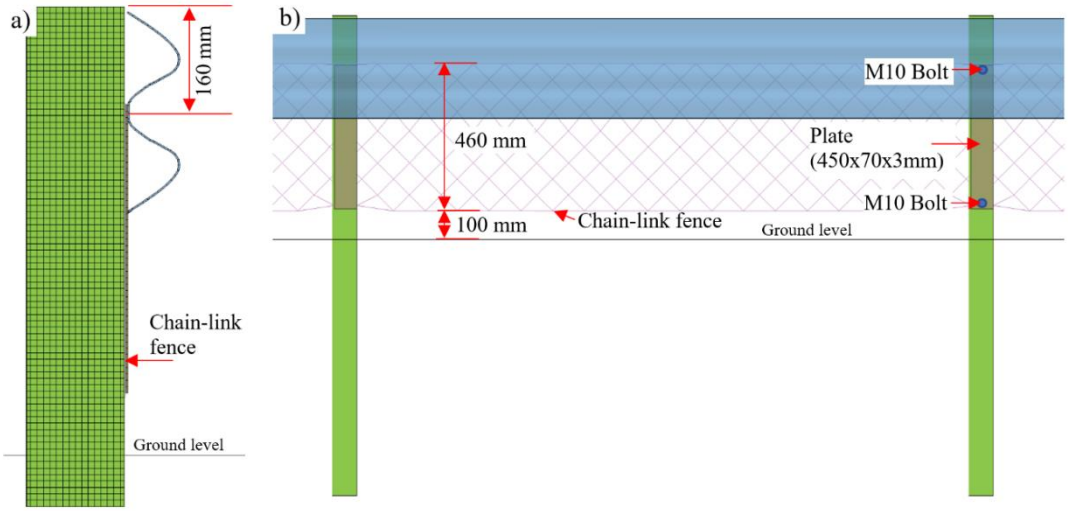


**Figure 8.** FE model of modified barrier system with fence: a) Side view, b) Front View

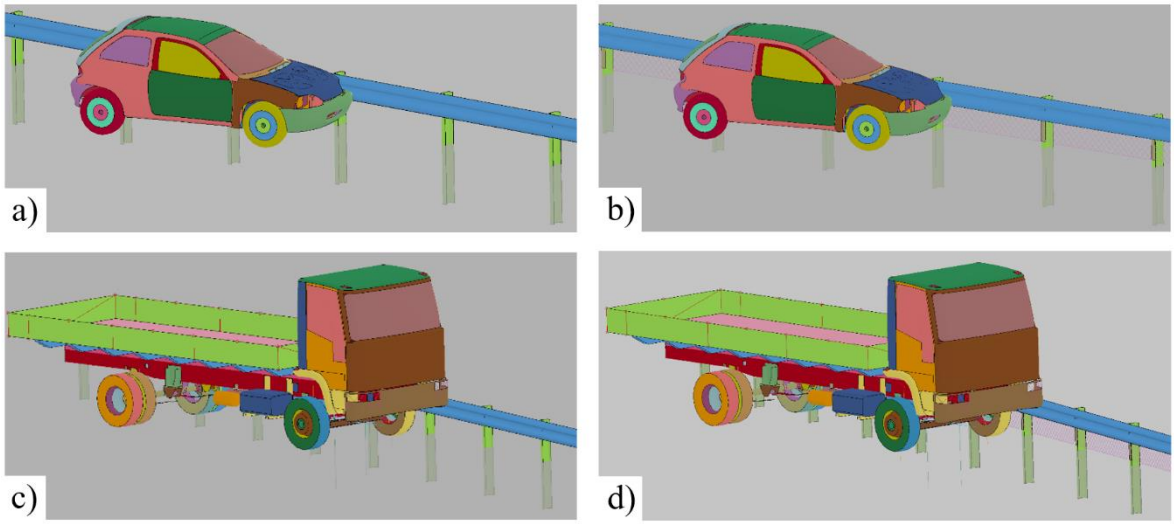


**Figure 9.** TB11 and TB42 FE model with and without fence: a) TB11 simulation without fence, b) TB11 simulation with fence, c) TB42 simulation without fence, d) TB42 simulation with fence

## 3. Results and Discussion

This study investigates the impact severity and barrier performance by analyzing the effect of chain-link fence attachment through FE analyses. Crash simulations were performed using the modified longitudinal barrier system, which was adjusted to reduce the weight of the certified H1 containment level barrier. TB11 and TB42 FE analyses were conducted for both the modified barrier system with and without chain-link fence attachment. The results of the FE simulations are presented and discussed in this section.

### 3.1. TB11 FE Analysis Results

TB11 crash test simulations were conducted for the modified longitudinal barrier, both with and without chain-link fence attachment. The FE analysis results were utilized to assess passenger impact severity and barrier performance. The evaluation employed ASI and THIV indices to determine impact severity levels, along with the assessment of barrier deformation under a car impact. The vehicle impacted the barrier at a speed of 100 km/h and an angle of 20°. Figure 10 illustrates the sequential comparison of TB11 crash test simulations for the modified safety barrier without and with chain-link fence placement. In both tests, 3 posts were detached from the rail due to the failure of M10 bolts. In both scenarios, the barriers effectively contained and redirected the 900 kg car, demonstrating the structural adequacy of the barrier.

Figure 11 shows the deformations in barriers resulting from the crash simulations. The working widths for cases without and with chain-link fence attachments were determined to be 0.72 m and 0.71 m, respectively. The conditions of the deformed region and working widths indicate that the chain-link fence had a minimal effect on the barrier's structural performance in the TB11 test.

In addition to structural evaluation, impact severities were also assessed for both cases. The ASI indices for the modified barrier system without and with a fence were determined to be 0.78 and 0.82, respectively. In both cases, the impact severity level is classified as A, indicating minimal injury risk to occupants. THIV results were calculated for the cases without and with fence placement as 22.8 and 24.7, respectively. Both results met the maximum THIV criteria specified in EN1217-2. Figure 12 presents a comparison of ASI graphs to demonstrate impact severity during crash testing time. FE analysis results indicated that while the implementation of the chain-link fence had a minimal effect on the TB11 test performance, it led to a slight increase in impact severity indices, still well within the EN 1317 limits.

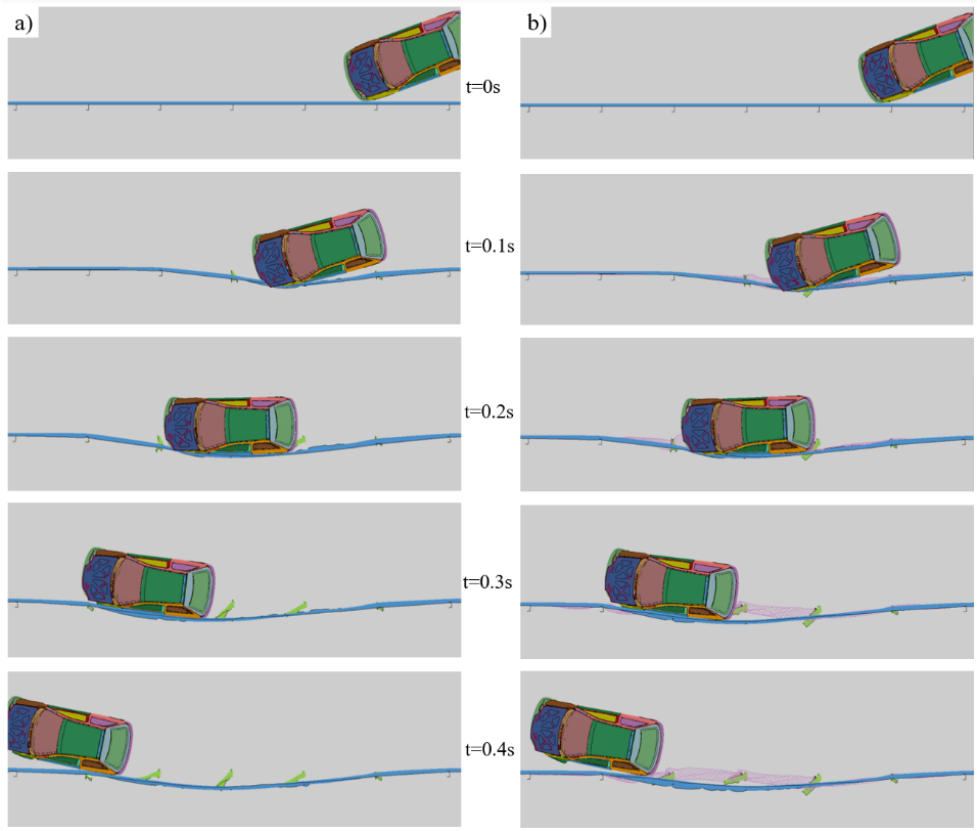


**Figure 10.** Comparison of TB11 simulations without and with fence: a) TB11 simulation without fence, b) TB11 simulation with fence

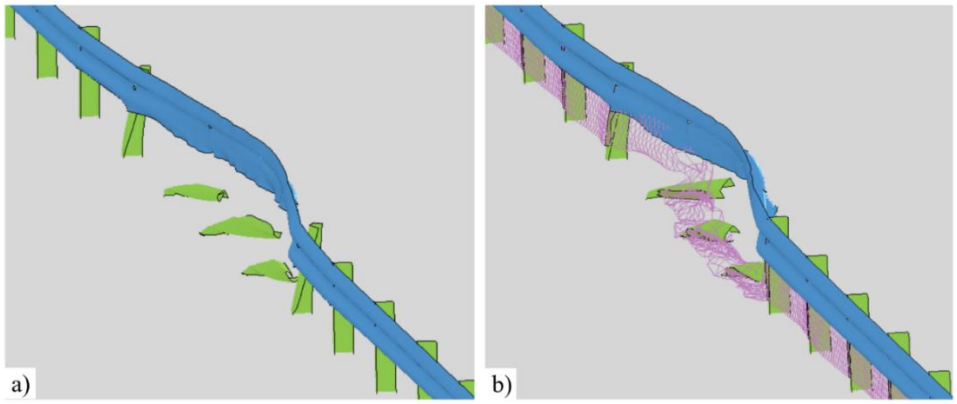


**Figure 11.** Damaged barriers after TB11 simulations: a) Barrier system without fence, b) Barrier system with fence

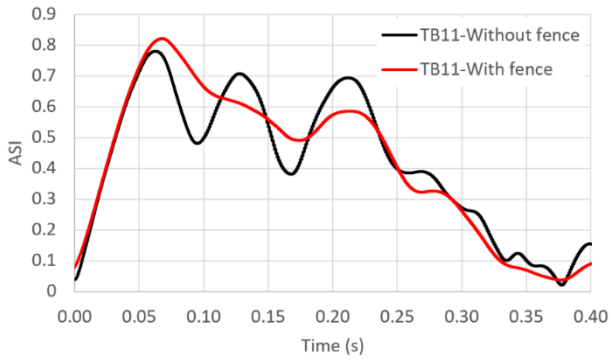


**Figure 12.** ASI graph comparison of two analyses

### 3.2. TB42 FE Analysis Results

TB42 crash simulations were conducted using an HGV model, evaluating the modified longitudinal barrier with and without chain-link fence attachment. The FE analysis results were employed to assess the barrier's structural adequacy in two different cases, examining damage and deformations in barrier components. The vehicle impacted the barrier at a speed of 70 km/h and an angle of 15°. Figure 13 presents a sequential comparison of TB42 crash test simulations for the modified safety barrier without

and with chain-link fence placement. In the case without the fence, the vehicle couldn't be contained and redirected by the modified barrier system. Following the impact, the system deformed, and at 0.35 seconds, the front wheel of the vehicle began to climb over the W-beam rail. Eventually, the vehicle overcame the barrier, passed to the back, and ruptured the rail. According to EN 1317-2, this test failed, and the modified barrier system without the fence did not meet H1 containment level requirements. In the second test, the modified barrier with fence attachment successfully contained and redirected the vehicle. After the initial impact, a total of 8 posts were detached from the rail due to the failure of M10 bolts. However, the barrier system functioned properly with the fence attachment, successfully redirecting the vehicle according to EN 1317-2. The working width of the safety barrier was determined to be 1.23 m, corresponding to the W4 working width class, the same as the initial reference heavier barrier system.

Figure 14 displays the final conditions of the barrier systems following the TB42 crash simulations. In the case of the modified barrier system without fence attachment, the vehicle could not be contained. A complete breakage in the longitudinal beam component occurred, resulting in test failure. In the second analysis, however, the presence of the chain-link fence strengthened the system, allowing the barrier to contain and redirect the vehicle successfully.

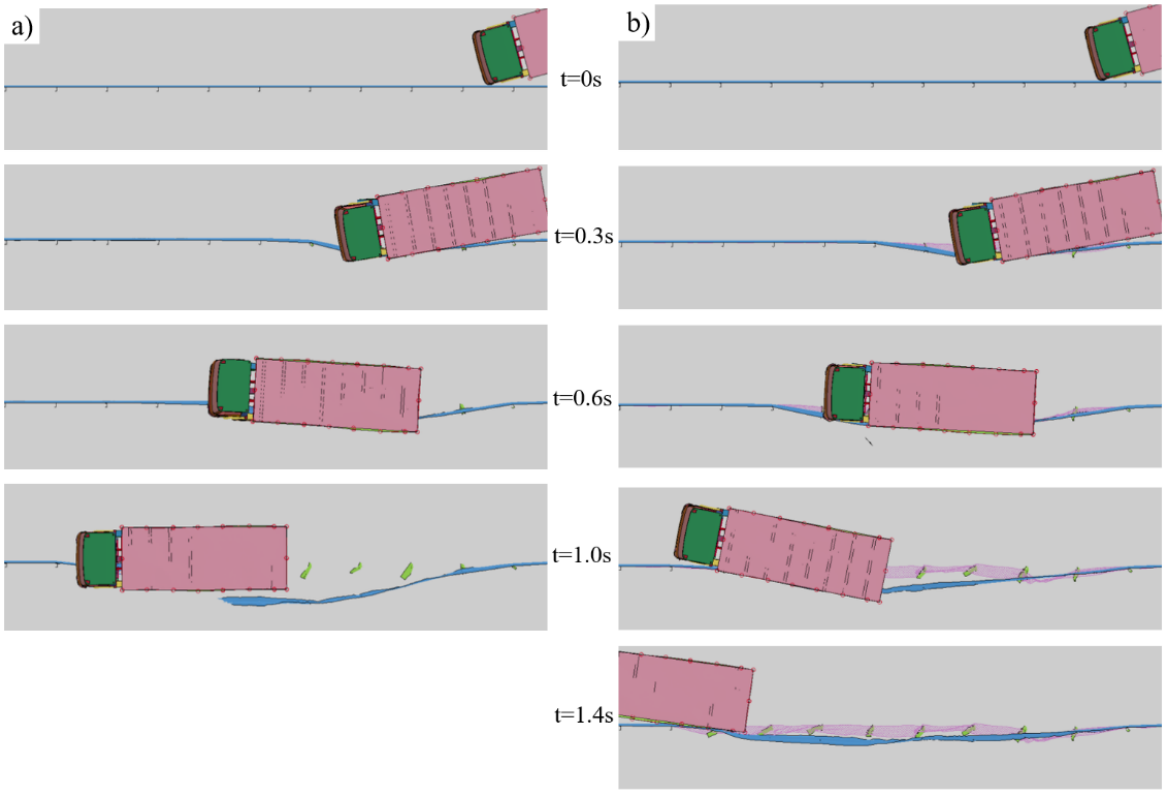


**Figure 13.** Comparison of TB42 simulations without and with fence: a) TB42 simulation without fence, b) TB42 simulation with fence

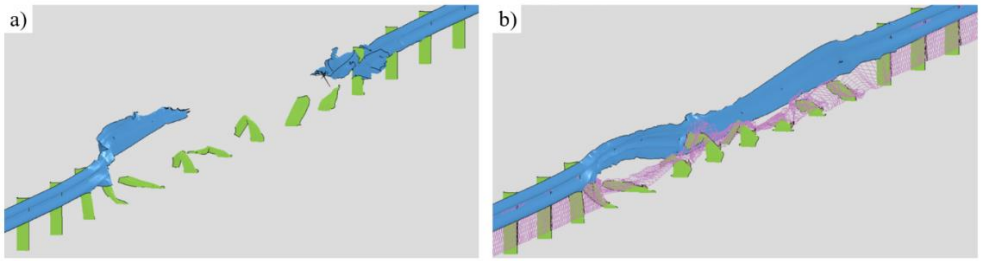


**Figure 14.** Damaged barriers after TB42 simulations: a) Barrier system without fence, b) Barrier system with fence

Table 4 provides a summary of the reference H1 barrier and the modified system crash test results, both with and without fence attachment. TB11 and TB42 FE analysis results demonstrated that the

modified longitudinal barrier systems, both without and with fence attachment, met the EN 1317 requirements for the TB11 test. However, the system without a chain-link fence failed in the TB42 crash test simulation. With the attachment of the chain-link fence to the modified barrier, it could effectively contain and redirect the HGV. These findings indicate that the reduced-weight modified barrier system, with the addition of the fence, achieved identical performance to the heavier reference H1-W4-A system. Consequently, chain-link fence attachment emerges as a viable alternative for strengthening existing barrier systems or incorporating into new barrier designs.

**Table 4.** The summary of test results

| Test | Parameter | Real test results of reference H1 barrier | Modified barrier without fence | Modified barrier with fence |
|---|---|---|---|---|
| TB11 | ASI | 1 | 0.78 | 0.82 |
| | THIV (km/h) | 23 | 22.8 | 24.7 |
| | Working width (m) | 0.73 | 0.72 | 0.71 |
| TB42 | Working width (m) | 1.14 | Failed | 1.23 |
| | Working width class | W4 | - | W4 |

## 4. Conclusion

In this study, the impact of chain-link fences on safety barrier performance in terms of impact severity and structural adequacy was investigated through numerical simulations. The numerical model underwent validation using real crash test results, and the validated reference H1 containment level barrier design was modified to reduce system weight. The modified system underwent TB11 and TB42 tests with and without chain-link fence attachment, leading to the following key findings:

- The FE model of H1 containment level barrier was successfully validated with real test results, confirming its suitability for further analyses.
- The attachment of the chain-link fence had minimal effect on TB11 test performance, resulting in a slight increase in impact severity indices that remained within EN 1317 limits.
- The modified barrier without chain-link fence attachment failed the TB42 test, while the system with chain-link fence attachment successfully contained and redirected the 10000 kg HGV in the TB42 test simulation.
- The modified barrier system with fence attachment demonstrated H1-W4-A performance, equivalent to the heavier initial reference system. The use of chain-link fences enhances the performance of a weaker barrier system by limiting the lateral movement of posts.

The results suggest that chain-link fences have the potential for use in improving the performance of existing longitudinal barriers or as a component to reduce system weight in new designs. Further studies, involving simulations and real full-scale crash tests with different containment level safety barriers, are recommended to thoroughly investigate the usability and effectiveness of chain-link fence systems.

## Conflict of Interest Statement

There is no conflict of interest between the authors.

## Statement of Research and Publication Ethics

The study is complied with research and publication ethics.

## References

[1] *Road restraint systems - Part 2: Performance classes, impact test acceptance criteria and test methods for safety barriers including vehicle parapets*, EN 1317-2, European Committee for Standardization, Brussels, Belgium, 2010.

[2] A. M. Molan, M. Moomen, and K. Ksaibati, "Investigating the effect of geometric dimensions of median traffic barriers on crashes: Crash analysis of interstate roads in Wyoming using actual crash datasets," *J. Safety Res.*, vol. 71, pp. 163–171, 2019.

[3] A. M. Molan and K. Ksaibati, "Impact of side traffic barrier features on the severity of run-off-road crashes involving horizontal curves on non-interstate roads," *Int. J. Transp. Sci. Technol.*, vol. 10, no. 3, pp. 245–253, 2021, doi: https://doi.org/10.1016/j.ijtst.2020.07.006.

[4] T.-L. Teng, C.-C. Liang, C.-Y. Hsu, C.-J. Shih, and T.-T. Tran, "Impact performance of W-beam guardrail supported by different shaped posts," *Int. J. Mech. Eng. Appl.*, vol. 4, no. 2, pp. 59–64, 2016.

[5] A. O. Atahan and A. O. Yucel, "Laboratory and field evaluation of recycled content sign posts," *Resour. Conserv. Recycl.*, vol. 73, pp. 114–121, 2013, doi: https://doi.org/10.1016/j.resconrec.2013.02.002.

[6] C. Silvestri-Dobrovolny, R. Bligh, M. Kiani, and A. Zalani, "Evaluation of Attachments to Concrete Barrier Systems to Deter Pedestrians—Volume 1: Technical Report," Texas, USA, No. FHWA/TX-23/0-7082-R1-Vol1, 2023.

[7] C. Silvestri-Dobrovolny, R. P. Bligh, M. Kiani, A. Zalani, W. J. L. Schroeder, and D. L. Kuhn, "Evaluation of Attachments to Concrete Barrier Systems to Deter Pedestrians—Volume 2: Crash Report," Texas, USA, No. FHWA/TX-23/0-7082-R1-Vol2, 2023.

[8] C. Silvestri Dobrovolny, S. Shi, J. Kovar, and R. P. Bligh, "Development and Evaluation of Concrete Barrier Containment Options for Errant Motorcycle Riders," *Transp. Res. Rec.*, vol. 2673, no. 10, pp. 14–24, 2019, doi: 10.1177/0361198119845900.

[9] T.-L. Teng, C.-C. Liang, and T.-T. Tran, "Effect of various W-beam guardrail post spacings and rail heights on safety performance," *Adv. Mech. Eng.*, vol. 7, no. 11, p. 1687814015615544, Nov. 2015, doi: 10.1177/1687814015615544.

[10] A. Ö. Yücel, A. O. Atahan, T. Arslan, and U. K. Sevim, "Traffic Safety at Median Ditches: Steel vs. Concrete Barrier Performance Comparison Using Computer Simulation," *Safety*, vol. 4, no. 4, 2018, doi: 10.3390/safety4040050.

[11] Z. Ren and M. Vesenjak, "Computational and experimental crash analysis of the road safety barrier," *Eng. Fail. Anal.*, vol. 12, no. 6, pp. 963–973, 2005, doi: https://doi.org/10.1016/j.engfailanal.2004.12.033.

[12] Ł. Pachocki and D. Bruski, "Modeling, simulation, and validation of a TB41 crash test of the H2/W5/B concrete vehicle restraint system," *Arch. Civ. Mech. Eng.*, vol. 20, no. 2, p. 62, 2020, doi: 10.1007/s43452-020-00065-7.

[13] A. O. Atahan, A. O. Yucel, and O. Guven, "Development of N2–H1 Performance-Level Guardrail: Crash Testing and Simulation," in *Transportation Research Circular, E-C172,* 2013.

[14] S. Tahmasbi, A. Giacomini, C. Wendeler, and O. Buzzi, "3D finite element modelling of chain-link drapery system," in *ISRM EUROCK*, ISRM, 2018, p. ISRM-EUROCK.

[15] T. T. Le Hoang, H. Masuya, Y. Nishita, and T. Ishii, "Experimental and numerical impact models of protection fences," *Int. J. Prot. Struct.*, vol. 11, no. 1, pp. 90–108, 2020, doi: 10.1177/2041419619852367.

[16] *Road restraint systems - Part 1: Terminology and General Criteria For Test Methods*, EN 1317-1, European Committee for Standardization, Brussels, Belgium, 2010.

[17] Transpolis SAS, "Barrier for Road edge and Median W-beam - TB11," TRANSPOLIS S.A.S., Saint-Maurice-de-Rémens, France, 2021.

[18] Transpolis SAS, "Barrier for Road edge and Median W-beam - TB42," TRANSPOLIS S.A.S., Saint-Maurice-de-Rémens, France, 2021.

[19] *LS-DYNA Keyword User's Manual*, LSTC, Livermore Software Technology Corporation: Livermore, CA, USA, 2012.

[20] *Road restraint systems - Validation and verification process for the use of virtual testing in crash testing against vehicle restraint system*, BS EN 16303:2020, BSI Standards Publication, 2020.

[21] *Finite element model archive*, NCAC, FHWA/NHTSA National Crash Analysis Center, George Washington University, Apr. 2008 [Online] Available: http:// www.ncac.gwu.edu/vml/models.html.

[22] Guneycelik, "Chain-link fence technical specifications," guneycelik.com.tr. https://www.guneycelik.com.tr/Tr/tel-orgu.html (accessed Jan. 1, 2024).

[23] Yapimtel, "Galvanized chain-link fence," yapimtel.com.tr. https://yapimtel.com.tr/urunler/galvaniz-orgu-teli/ (accessed Jan. 1, 2024).

[24] *Steel wire and wire products for fencing and netting - Part 6: Steel wire chain link fencing*, TS EN 10223-6, Turkish Standard, Turkish Standards Institution, Ankara, 2013.

[25] Te-fence, "Chain-link fence," te-fence.com. https://te-fence.com/chain-link-fence/ (accessed Jan. 1, 2024).